AIP Conference Proceedings

The Magnetic Structure of $RbMnBr_3$

Cite as: AIP Conference Proceedings **10**, 659 (1973); https://doi.org/10.1063/1.2946987
Published Online: 03 July 2008

C. J. Glinka, V. J. Minkiewicz, D. E. Cox, and C. P. Khattak

View Online Export Citation

ARTICLES YOU MAY BE INTERESTED IN

Spin waves in the triangular antiferromagnet $CsMnBr_3$
Journal of Applied Physics **61**, 3409 (1987); https://doi.org/10.1063/1.338762

Lock-in Amplifiers up to 600 MHz
Zurich Instruments
Watch

© 1972 American Institute of Physics.

THE MAGNETIC STRUCTURE OF $RbMnBr_3$

C. J. Glinka and V. J. Minkiewicz*
University of Maryland, College Park, Maryland 20742

D. E. Cox**
Brookhaven National Laboratory, Upton, N.Y. 11973

C. P. Khattak
SUNY at Stonybrook, N.Y. 11790
and Brookhaven National Laboratory, Upton, N.Y.

ABSTRACT

The magnetic properties of the $CsNiCl_3$-type compound $RbMnBr_3$ have been studied by powder neutron diffraction and susceptibility measurements. Below $T_N = 8.8 \pm 0.1°K$, the compound exhibits antiferromagnetic order. The Mn^{+2} moments lie parallel to the basal plane of the hexagonal lattice and form antiferromagnetic chains along the c axis. In the basal plane the spins form a spiral which differs from the simple triangular arrangement found in other compounds of this type in that the turn angle is about 130° rather than 120°. The Mn^{+2} moment extrapolated to 0°K is $3.6 \pm 0.15\mu_B$. This large reduction in the magnetic moment is believed to reflect strong zero-point spin wave deviation. Similar reduction of the Ni^{+2} moment has been observed in $CsNiCl_3$ and $RbNiCl_3$.

INTRODUCTION

$RbMnBr_3$ is one of a class of isostructural ABX_3 compounds which have received extensive study recently as a result of their quasi one-dimensional magnetic properties.[1] In these compounds the $(BX_3)^{-1}$ complexes form closely linked chains of octahedra along the c-axis of the hexagonal lattice. The one-dimensional character arises primarily because these chains are widely spaced in the basal plane with the result that the transition metal ions, Mn^{+2} in the present case, are separated by about 7Å in the basal plane and by only 3Å along the c-axis.

Neutron diffraction measurements were performed on a powder sample of $RbMnBr_3$ using a triple-axis spectrometer. Graphite crystals were used in both the monochromator and analyzer positions with their (002) planes oriented to Bragg reflect the same wavelength so that only elastically scattered neutrons were finally detected. In this way both the peak-to-background ratio and the angular resolution were enhanced without serious reduction in intensity. A wavelength of 2.46Å was employed to further improve the resolution of the powder patterns. The $\lambda/2$ component at this wavelength was selectively scat-

*Work supported by NSF.
**Work supported by U.S. Atomic Energy Commission.

tered out of the beam by a high efficiency pyrolytic graphite filter.[2]

CHEMICAL STRUCTURE

$RbMnBr_3$ was prepared by evaporation of a hydrobromic acid solution of reagent grade Rb and Mn carbonates, followed by melting in an atmosphere of anhydrous HBr. As far as could be ascertained the compound has not previously been reported. It was found to be isostructural with $CsNiCL_3$, which has the hexagonal space group $P6_3/mmc$ (D^4_{6h}). There are two formula units in the primitive cell which has lattice constants a = 7.36 Å and c = 6.52 Å at 4.5°K. The Rb^{+1} ions are at the positions (1/3,2/3,1/4) and (2/3, 1/3,3/4), the Mn^{+2} ions occupy the (0,0,0) and (0,0,1/2) sites, while the Br^{-1} ions are at $\pm$ (x,2x,1/4), $\pm$ (x,$\bar{x}$,1/4) and $\pm$ ($2\bar{x}$,$\bar{x}$,1/4). Intensities calculated with x = 0.164 are compared in Table I with those observed for a room temperature scan. Several peaks which could not be indexed appeared in the room temperature data and remained unchanged over the entire temperature range investigated and so are believed to be due to non-magnetic impurities. The impurity content was estimated to be about 5% from the relative intensities.

Table I Comparison of observed and calculated nuclear intensities for $RbMnBr_3$ at room temperature.

hkl	I_{OBS}(RT)	I_{CAL}
(100)	545	528
(101)	10	8
(110)	140	148
(002) (200)	5220	5330
(201) (102)	7430	7299
(112) (210)	360	320
(202) (211)	590	653
(300)	30	36
(103)	10	1
(220)	925	1003

$R = \sum |I_{OBS} - I_{CAL}| / \sum I_{OBS} = 0.03$

MAGNETIC STRUCTURE

All of the magnetic structures previously found for $CsNiCl_3$-type compounds have been commensurate with an enlarged hexagonal unit cell with dimensions $\sqrt{3}a \times \sqrt{3}a \times c$, where a and c refer to the fundamental chemical cell. The a axis of this magnetic cell makes an angle of 30° with the a axis of the chemical cell. Figure 1 shows a diffraction pattern of $RbMnBr_3$ obtained at T = 4.5°K. The results of scans of the three prominent magnetic peaks in this figure are shown in Fig. 2. Indicated in these figures are the positions of magnetic peaks of the enlarged magnetic cell indexed on the fundamental chemical cell. The data in these figures show that in contrast to the single diffraction peak usually observed for compounds of this type there occur multiple peaks displaced by varying amounts from the predicted positions. If this splitting is ignored, the combined intensities of each set of multiple peaks closely fit those calculated from a triangular model like that found for other

$CsNiCl_3$-type compounds. In this model the spins lie within the basal plane and alternate along the c axis forming antiferromagnetic chains. The spins in the basal plane form a spiral with a turn angle of 120°.

The observed splitting of the magnetic peaks can be understood as arising from a modification of the triangular model in which the spiral turn angle deviates from 120° by some small angle θ. The propagation vector of this more general structure is

$$\vec{\tau} = (1/3 + \theta/2\pi)\vec{a}^* + (1/3 + \theta/2\pi)\vec{b}^* \qquad (1)$$

where a* and b* are reciprocal basis vectors of the chemical cell.

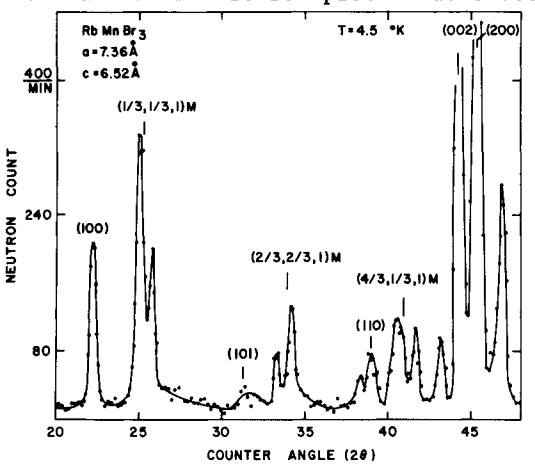

Fig. 1 Neutron diffraction pattern of $RbMnBr_3$. Indexing is based on the primitive chemical cell. Magnetic peaks are designated by the letter M. The peaks at 38.2, 43.3° and 46.8° could not be indexed but were observed to be non-magnetic.

The spin configuration generated by Eq. 1 is depicted in Fig. 3. The propagation vector of the triangular model is a special case of Eq. 1 for θ = 0. The magnetic scattering vectors, $\vec{Q}$, are related to the propagation vector $\vec{\tau}$ by

$$\vec{Q}_{\pm} = \vec{G}_{hkl} \pm \vec{\tau} \qquad (2)$$

where $\vec{G}_{hkl}$ is a nuclear reciprocal lattice vector and where ℓ is odd. From Eqs. 1 and 2 it is seen that for the triangular model (θ=0) the scattering vectors $\vec{G}_{001} + \vec{\tau}$, $\vec{G}_{101} - \vec{\tau}$ and $\vec{G}_{011} - \vec{\tau}$, for example all have the same magnitude and therefore contribute to a single magnetic peak with indices (1/3,1/3,1). If θ is greater than zero, however, the length of the scattering vector $\vec{G}_{001} + \vec{\tau}$ is increased while the lengths of the vectors $\vec{G}_{101} - \vec{\tau}$ and $\vec{G}_{011} - \vec{\tau}$ are decreased by equal amounts. As a result the (1/3,1/3,1) peak of the triangular model is split into two components; the multiplicity of the component shifted downward is twice that of the component shifted upward in angle. The splitting and relative intensities of the other magnetic peaks shown in Figs. 1 and 2 can be accounted for in a similar fashion. The positions of the magnetic peaks in these figures are also correctly given by the modified model for $\theta = 8.5 \pm 1.4°$.

Integrated intensities calculated from both the modified and unmodified triangular models are compared with experimental values in Table II. The positions of the magnetic peaks derived from the two models are also compared in the table. The table shows that the triangular model would fit the data very well if the splitting of the

magnetic peaks were not resolved. It is this splitting that is the essential feature of the data which establishes the modified triangular model as the correct structure. As noted in Table II, the data can best be fit for a strikingly low value for the Mn^{+2} moment of only $3.3\mu_B$.

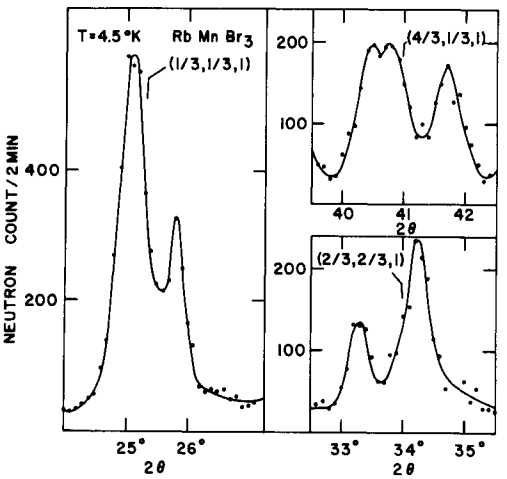

Fig. 2 Detailed structure of the magnetic peaks shown in Fig. 1. The indices and indicated positions are those predicted by the triangular model.

Finally Fig. 4 illustrates the results of susceptibility measurements on a poly-crystalline sample of $RbMnBr_3$ as a function of temperature. The broad minimum in χ_M^{-1} shown in the figure is similar to that often observed for such compounds and is characteristic of linear antiferromagnetic chains.[1] The sharp break in χ_M^{-1} near 10°K marks the transition to three-dimensional order. The transition temperature was more precisely determined from the temperature dependence of the magnetic diffraction peaks to be $T_N = 8.8 \pm 0.1$°K. Fisher[3] has calculated the susceptibility of a linear chain for the

Table II Comparison of observed magnetic intensities with those calculated for the triangular and modified triangular models. The intensities are designated by the peak positions shown in Fig. 2.

		Modified Model		Triangular Model	
$2\theta_{OBS}$	I_{OBS}(4.5°K)	$2\theta_{CAL}$	I_{CAL}	hkl	I_{CAL}
25.1°	131	25.1°	124	(1/3,1/3,1)	183
25.8°	53	25.8°	57		
33.3°	21	33.2°	26	(2/3,2/3,1)	73
34.2°	53	34.3°	47		
40.5°	56	40.4°	55	(4/3,1/3,1)	81
40.8°		40.8°			
41.7°	22	41.7°	25		
		$\mu = 3.3\mu_B$		$\mu = 3.4\mu_B$	

infinite spin case. Applying the results of the calculation to $RbMnBr_3$, the data in Fig. 4 yield an exchange constant of $J_s = 12°K$ between the Mn^{+2} ions along the c-axis. The magnetic intensity data, when extrapolated to 0°K, give a limit value for the Mn^{+2} moment of only $3.6 \pm 0.15\mu_B$. This large reduction in the magnetic moment is believed to reflect strong zero-point spin wave deviation[4]. Similar effects were observed in studies of $CsNiCl_3$[5] and $RbNiCl_3$[6] which resulted in values for the Ni^{+2} moment of $1.05\mu_B$ and $1.30\mu_B$ respectively.

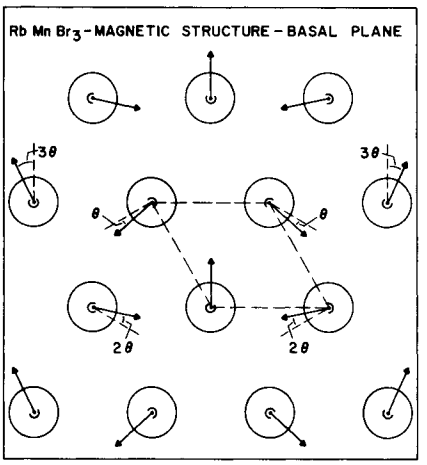

Fig. 3 The basal plane of the magnetic structure of $RbMnBr_3$ showing the fundamental chemical cell. The angle θ measures the departure of the moment directions from those of the triangular model.

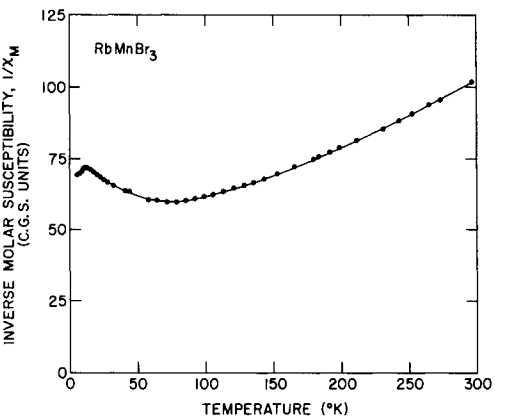

Fig. 4. Inverse molar susceptibility of $RbMnBr_3$ as a function of temperature.

The occurrence of a modulated arrangement incommensurate with a simple multiple of the chemical cell is rather surprising. It may be contrasted with the ideal triangular structure observed in $CsMnBr_3$[7], and presumably reflects some subtle difference in more distant neighbor exchange interactions.

REFERENCES

1. N. Achiwa, J. Phys. Soc. Japan 27, 561 (1969).
2. B. O. Loopstra, Nucl. Instrum. Methods 44, 181 (1966).
3. M. E. Fisher, Am. J. Phys. 32, 343 (1964).
4. P. A. Montano, E. Cohen, and H. Shechter, Phys. Rev. B6, 1053 (1972).
5. D. E. Cox and V. J. Minkiewicz, Phys. Rev. B4, 2209 (1971).
6. W. B. Yelon and D. E. Cox, Phys. Rev. B6, 204 (1972).
7. M. Eibschutz, R. C. Sherwood, F. S. L. Hsu, and D. E. Cox, AIP Conference Proceedings, Magnetism and Magnetic Materials 1972.